

# ELECTROCHEMICAL STUDIES ON TRIBOCORROSION BEHAVIOR OF A NICKEL-CHROMIUM-MOLYBDENUM DENTAL ALLOY IN ARTIFICIAL SALIVA

Alexandra BANU,<sup>a</sup> Maria MARCU<sup>b\*</sup> and Octavian RADOVICI<sup>a</sup>

<sup>a</sup> Politehnica University from Bucharest, Faculty of Engineering of Management of Technological Systems, Splaiul Independentei 313, 060042, Bucharest, Roumania

<sup>b</sup> Institute of Physical Chemistry “Ilie Murgulescu”, Splaiul Independentei 202, 060021, Bucharest, Roumania

Received December 18, 2007

Tribocorrosion of metals and alloys involves the simultaneous action of corrosive solution and a mechanical stress. Anodic behavior of Chromium-Molybdenum alloys under friction and wear in artificial saliva solution were carried out. It was found that electrochemical characteristics of CrMo alloy (rest potential, rate of anodic dissolution) are not decisively influenced by straining and plastic deformation. It was concluded that friction and wear of dental alloy does not change their corrosion resistance during mastication.

## INTRODUCTION

Surface engineering is becoming increasingly important in the dental alloys sector as a means of achieving the desired surface properties in terms of friction and wear in an economic manner. The term mechano-electrochemical effect has been used to describe relationship between mechanical factors particularly the effect of stress in the application of a material, and the electrochemical responses especially.<sup>1</sup> It has become apparent that in order to optimize tribological performance of dental alloys, a contribution of surface corrosion and lubrication engineering is required.

In this paper the anodic film formation is assessed at a chromium alloy's surface under friction and wear.

## EXPERIMENTAL

Experiments were conducted using a Nickel-Chromium-Molybdenum (NiCrMo) dental alloy with the following chemical composition (Table 1).

Table 1

Chemical composition of casting dental alloy (% weight)

Cr, %	Mo, %	Si, %	Mn, %	Ti, %	Ni, %
27.97	4.23	0.92	0.6	0.42	base

The samples were cut off from a casting alloy and wear surface was obtained using a pin-on plate apparatus instrumented to measure the frictional force via a bi-directional load cell.<sup>2,3</sup> The contacting surface of the pin was 0.15 cm<sup>2</sup>. Pin was fabricated from the same alloy as the test alloys. Wear tests have been carried out on the apparatus described above under lubricated conditions using artificial saliva solution.<sup>4</sup> A constant load of 7.33 N/mm<sup>2</sup> was applied in the tests reported here, the parameters of the test were Normal force [N/mm<sup>2</sup>], Medium rate [mm/min] and Friction force [N/mm<sup>2</sup>].

### Electrochemical experiments

All the electrochemical experiments were carried out in artificial saliva solution in stagnant and rotating conditions, in presence of SiC as an abrading material. The abrasive medium comprised SiC (4μ diameter) particles uniformly distributed in the volume of stirred artificial saliva solution (Fusayama Meyer).<sup>4</sup> The rotating speed of solution was 500, 1000 and 1500 rot/min.

All measurements were performed in a glass cell provided with a platinum net counter-electrode and a SCE electrode as a reference electrode. The working electrode (WE) was a NiCrMo alloy rod (for chemical composition see Table 1) with an exposed area of 0.7cm<sup>2</sup>. Prior to each measurement electrodes were mechanically polished with abrasive paper. After a treatment in an ultrasonic bath with ethanol the electrode was removed from the bath and rinsed with bidistilled water. Electrochemical measurements were performed immediately after strain test. To reduce the surface relaxation of the samples, the SiC containing electrolyte was stirred.

Potentiodynamic polarization curves were carried out in the potential range from -1.0V to 1.0V with a scan rate of

\* Corresponding author: m\_marcu2000@yahoo.com

10 mV/sec. Cyclic voltammetry curves were obtained in a potential range of  $-1.0\text{V}$  to  $1.0\text{V}$  with a scan rate of 100, 200 and 500 mV/sec. Open circuit potential was determined in stagnant and stirred conditions for 24 hours.

## RESULTS AND DISCUSSION

The testing parameters for the surface wear, friction force and the surface's Profilogramme are presented in the Table 2 and Fig. 1.

Mecano-electrochemical effects describe relationships between mechanical forces applied on the material's surface and the electrochemical responses. The major concern of the field is the effect of stress (deformation) on the electrochemical properties of the metallic material, especially the open circuit electrode potential (OCP) and the kinetics of the electrode processes.<sup>5,6</sup>

Table 2

Testing parameters and the friction force

Normal force = $7.33\text{ N/mm}^2$		Friction force ( $\text{N/mm}^2$ )	
Medium rate (mm/min)		Maximum	Minimum
Right	0,633	45	30
Left	1	60	50
	0.692	100	60
	1	110	80

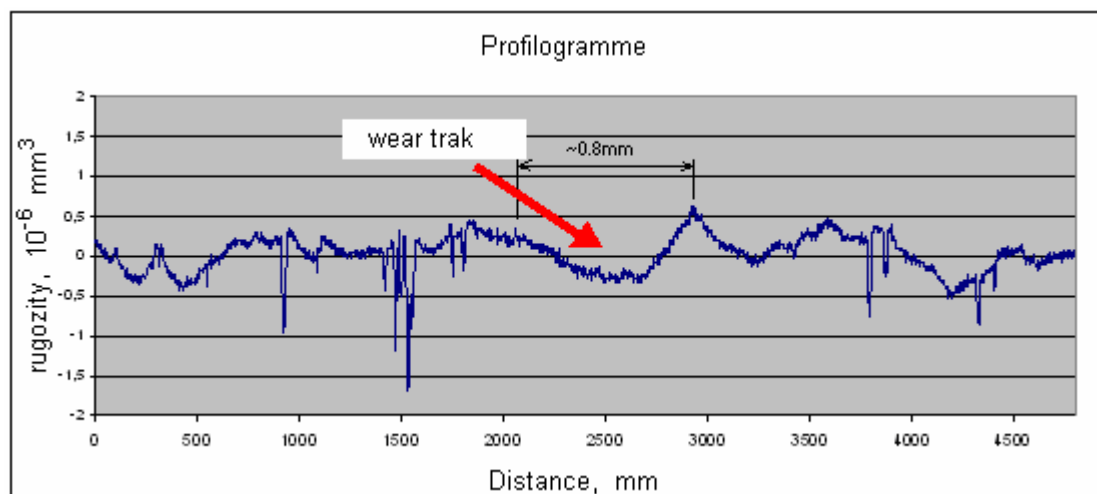


Fig. 1 – The sample's profilogramme during strain test.

### Open circuit potential (OCP)

The effects of friction (plastic deformation) on the OCP were discussed by Lewis *et al.*<sup>7,8</sup> which pointed out that the difference in surface free energy and hence electrode potential ( $\phi$ ) is directly related to the strain free energy  $\Delta G_{\text{strain}}$ .

$$\Delta\phi = -k\Delta G_{\text{strain}} \quad (1)$$

In agreement with this equation, the OCP of strained electrode (which presents excess strain surface energy) are displaced toward more active (negative) values as is shown in Fig. 2.

Also, was shown that the potential changes were transient. Thus straining the alloys into plastic region produced potential's changes starting in some alloy only during straining or for other alloy over long periods of time.

The electrode potential changes of NiCrMo alloys under plastic deformation (under stress) and in normal (not deformed) state are presented in Fig. 2.

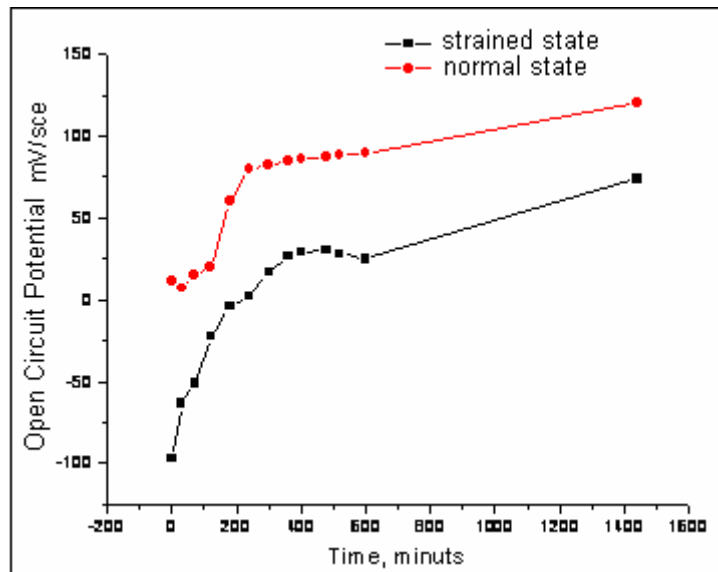


Fig. 2 – Time variation of Open Circuit Potential for both samples (normal state and under plastic deformation) in artificial saliva without SiC.

The OCP data presented in Fig. 2 shows that the wear process induced by friction produce the activation of surface of alloy, as well as the slow repassivation as the results of strain relaxation process comparing with simultaneously straining measurements when the depassivation process move the OCP of dental alloy to more electronegative values.<sup>6</sup>

### Polarisation curves

Figs. 3 and 4 show the cyclic potentiodynamic polarization curves of NiCrMo electrodes in unstrained and strained condition. Also the experiments were carried out in artificial saliva solution under stagnant and under hydrodynamic flow condition.

The principal electrochemical parameters of the anodic polarisation  $I_{cr}$ ,  $\phi_{cor}$ ,  $\phi_{i0}$ ,  $I_p$  are presented in Tables 3 and 4.

The data presented in Tables 3 and 4 show higher negative value  $\phi_{i0}$ ,  $\phi_{cr}$  for unstrained electrodes than for the strained (plastically deformed) electrodes, higher critical current density for the same electrodes and similar values of  $i_p$  always persisting. Also we stress that the most important control factors of the electrochemical parameters are hydrodynamic flow condition and in a much lesser extent the strain factor; *i.e.*  $\phi_{i0}$ ,  $\phi_{cr}$  and  $i_{cr}$  are controlled by the amounts of oxidizing and reducing species and the hydrodynamic solution flow conditions.  $\phi_{i0}$  can be also affected by the conductivity of the oxide films formed on metal surfaces in aqueous environments.

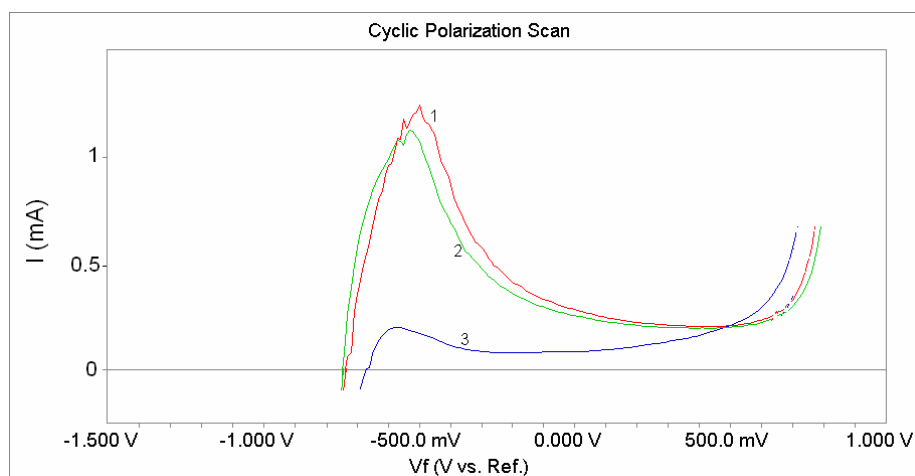


Fig. 3 – The polarization curves of normal samples at different rotation speed in artificial saliva with SiC. (1), 1500rot/min; (2), 1000 rot/min; (3), 0 rot/min.  $A=1 \text{ cm}^2$ .

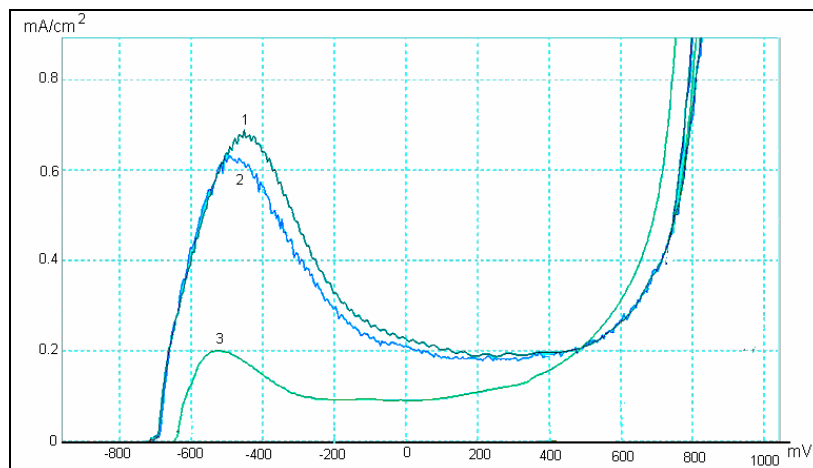


Fig. 4 – The polarization curves of frictioned samples at different rotation speed in artificial saliva with SiC: (1), 1500rot/min; (2), 1000 rot/min; (3), 0 rot/min.

Table 3

Parameters for non strained samples

Hydrodynamic condition	$\varphi_{i0}$ (mV)	$\varphi_{cr}$ (mV)	$i_{cr}$ ( $\mu$ A)	$i_p$ ( $\mu$ A)
stagnant	-666	-577	200	100
1000 rot /min	-743	-485	1077	195
1500 rot /min	-736	-500	1700	210

Table 4

Electrochemical parameters for strained samples

Hydrodynamic condition	$\varphi_{i0}$ (mV)	$\varphi_{cr}$ (mV)	$i_{cr}$ ( $\mu$ A)	$i_p$ ( $\mu$ A)
0	-650	-550	200	100
1000 rot /min	-715	-480	680	200
1500 rot /min	-706	-500	620	200

No control of straining and hydrodynamic flow on  $i_p$  was observed, which means that in passive region the kinetic control is the dissolution of the passive film under the condition of the presence of Cl<sup>-</sup> ions. Most likely to dissolve is nickel oxide as a component of the film.

### Effect of the flow rate

It has been reported that  $\varphi_{i0}$  is altered by hydrodynamic solution flow conditions. The mass

$$i = zFk_r C_0^x \exp\left[\frac{\varphi - \varphi_o}{b_0}\right] - nFk_{ox} C_2^x \exp\left[-\frac{\varphi - \varphi_o}{b_2}\right] \quad (2)$$

The mass-transport kinetics comes into play if the surface transfer reaction rates are very fast.

Thus the current associated with the first term of equation (2) can be expressed in terms of the concentration gradient in the boundary layer at the electrode surface

transfer rate of reactant from the bulk to the metal surface depends on the hydrodynamic conditions and hence on diffusion layer thickness  $\delta$ , which decreases with increasing the hydrodynamic flow.

Because  $\varphi_{i0}$  is the mixed potential associated with the kinetic balance between the two redox reactions occurring on an alloy surface it can be expressed by the known Butler- Volmer equation:

$$i = \frac{zFD(C_b - C_s)}{\delta} \quad (3)$$

where D is the diffusion coefficient of the oxidant,  $C_b$  is the concentration of the oxidant in the bulk,

$C_s$  is the oxidant concentration on the surface,  $\delta$  is the diffusion layer thickness.

$$i = zFk_0 \left( \frac{i\delta}{zFD} + C_s \right) - \exp \left[ \frac{(\varphi - \varphi_0)}{b_0} \right] \quad (4)$$

First term of equation (4) shows the influence of hydrodynamic flow on the  $I_{cr}$ .

In Fig. 5 which presents the electrochemical impedance spectra in a Nyquist plot (a) and Bode plot (b), one can notice the depressed semicircle in the Nyquist plot at high frequency, as well as

Rearranging equation coefficient and substituting in the first term of equation (2) (reaction order  $\geq 1$ ) gives:

Warburg-type impedance at low frequencies which characterize a passive electrodes surface. These data suggest that the rate determining step in the corrosion mechanism is diffusion through the passive film.

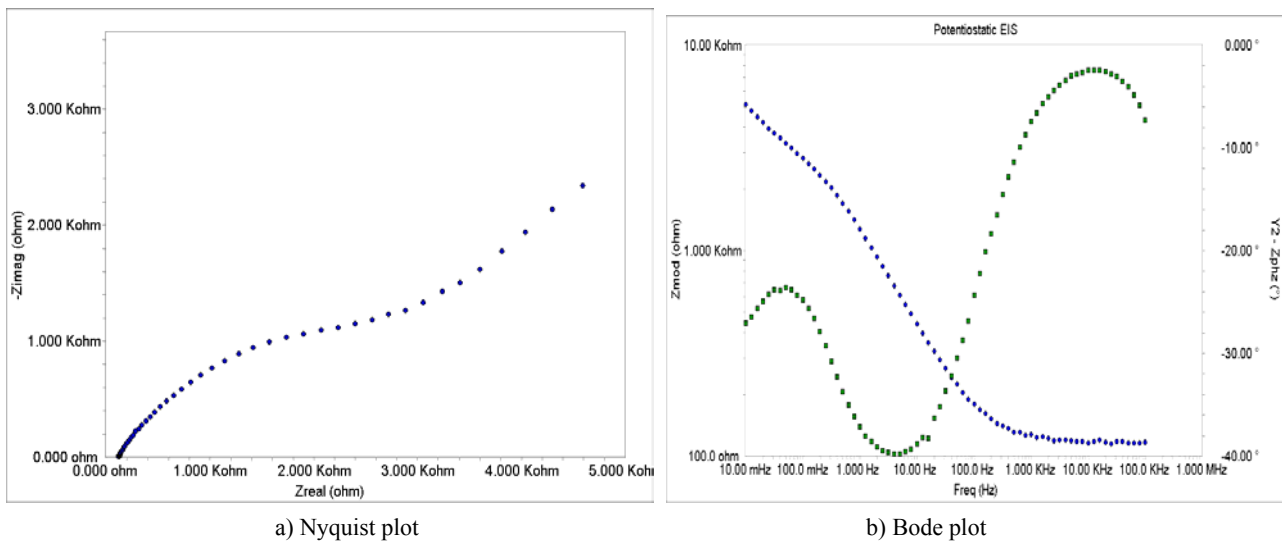


Fig. 5 – The EIS spectra of frictioned sample in artificial saliva.

### Effect of straining

This behaviour can be explained on the basis of the mechanism of plastic deformation of metals by slipping along particular crystal planes.<sup>9</sup>

Considerable differences in the extent of increase of the dissolution rate upon straining among different metals can be understood taking into account that some metals develop high index planes upon slipping while other do not. Conclusion is that the metals and alloys which do not develop high index plane (NiCrMo alloy, etc.) do not influence significantly the dissolution rate.

### CONCLUSIONS

Straining and plastic deformation of NiCrMo alloys produce small but distinct differences in the reversible potentials, rest potentials, rate of anodic

dissolution compared to well equilibrate randomly oriented metals.

The changes are rather insignificant so that the straining and wear of the NiCrMo dental alloys during mastication have not an important influence on their corrosion in neutral biofluids.

### REFERENCES

1. R.G. Raicheff, A. Damianovich and J. O'M. Bockris, *J. Chem. Phys.*, **1967**, 47, 219.
2. M.C. Gaspar and A. Ramalho, *Wear*, **2002**, 252, 199-209.
3. K. Zhang and L. Battiston, *Wear*, **2002**, 252, 332-344.
4. J. M. Meyer, J. N. Nally, *J. Dent. Res.*, **1975**, 54, 157.
5. T.P. Hoar and J.G. Heines, *J. Iron Steel Inst.*, **1956**, 182, 124.
6. Y. Yan, A. Neville and D. Dowson, *Wear*, **2007**, 263, 1417.
7. T.P. Hoar and J. M. Warst, *Proc. Roy. Soc.*, **1962**, A 286, 304.
8. D. Lewis and C. E. Pearce, *Electrochim. Acta*, **1971**, 16, 742.
9. M.A. Devanathan and M.J. Fernando, *Electrochim. Acta*, **1970**, 15, 1623.

